AJNR

Cerebellar Vermian Atrophy after Neonatal Hypoxic-Ischemic Encephalopathy

Michael A. Sargent, Kenneth J. Poskitt, Elke H. Roland, Alan Hill and Glenda Hendson

AJNR Am J Neuroradiol 2004, 25 (6) 1008-1015
http://www.ajnr.org/content/25/6/1008

Cerebellar Vermian Atrophy after Neonatal Hypoxic-Ischemic Encephalopathy

Michael A. Sargent, Kenneth J. Poskitt, Elke H. Roland, Alan Hill, and Glenda Hendson

BACKGROUND AND PURPOSE: **Although pathologic evidence of cerebellar injury due to birth asphyxia is well described, neuroimaging evidence is sparse. The primary purpose of this retrospective study was to evaluate the early and late imaging findings in the cerebellum of patients who had neonatal hypoxic-ischemic encephalopathy with thalamic edema shown by neonatal CT. The secondary aims were to validate thalamic edema shown by neonatal CT as a marker of thalamic injury and to assess the late cerebral cortical abnormalities associated with neonatal thalamic edema.**

METHODS: **Fifty-five neonates with thalamic edema shown by CT performed when patients were 3 days old were identified from a cohort of full-term neonates with hypoxic-ischemic encephalopathy. Twenty-six of the 55 underwent follow-up neuroimaging. All sonograms, CT scans, and MR images of the brains of the 55 neonates were retrospectively reviewed by two pediatric neuroradiologists. The examinations were reviewed for evidence of hemorrhage, edema, atrophy, and CT attenuation or MR signal intensity abnormalities in the cerebellum, basal ganglia, and cerebral cortex. The neonatal autopsy findings in four cases were reviewed separately by a pediatric neuropathologist.**

RESULTS: **Of the 55 neonates with thalamic edema shown by neonatal CT, 28 (51%) had thalamic edema with diffuse cerebral cortical edema, and 27 (49%) had thalamic edema without diffuse cortical edema. The cerebellar vermes appeared normal on all neonatal sonograms, CT scans, and MR images. However, atrophy of the cerebellar vermis was found in 12 (46%) of 26 patients by use of follow-up studies (95% CI, 27−65%). One of the 12 patients also had cerebellar hemispheric atrophy. Cerebellar vermian atrophy was shown at follow-up in eight (67%) of 12 patients who had neonatal thalamic edema with cortical sparing, compared with four (29%) of 14 patients who had thalamic edema with diffuse cortical edema. The difference did not reach statistical significance. The thalami appeared abnormal on follow-up neuroimages in 25 of 26 cases. Different patterns of cortical atrophy were observed on the images of patients who had thalamic edema with cortical sparing compared with those obtained in patients who had thalamic edema with cortical involvement.**

CONCLUSION: **Cerebellar vermian atrophy is a frequent finding on follow-up images of patients in whom neonatal CT showed hypoxic-ischemic encephalopathy with abnormal thalami.**

Studies using radio-labeled microspheres in lambs and fluorine-18-fluorodeoxyglucose positron emission tomography in infants have shown regional differences in perfusion and metabolic activity for glucose in the normal brain. The most active sites include the thalami and basal ganglia, sensorimotor (perirolandic) cortex, cerebellar vermis, and brain stem (1–3).

The clinical neurologic syndrome observed in patients with suspected birth asphyxia is commonly referred to as hypoxic-ischemic encephalopathy, because the relative contributions of hypoxia, ischemia, and other factors are usually unknown. Two major patterns of injury are typically identified in full-term neonates with hypoxic-ischemic encephalopathy (4). In one, diffuse cortical injury is present with relative sparing of the thalami and basal ganglia, which classically leads to multicystic encephalomalacia. This pattern is most commonly associated with prolonged

Received October 17, 2002; accepted after revision November 17, 2003.

Presented at the annual meeting of the Radiological Society of North America, Chicago, November 2000.

From the Departments of Radiology (M.A.S., K.J.P.) and Pathology (G.H.) and the Division of Neurology (E.H.R., A.H.), British Columbia's Children's Hospital, Vancouver, British Columbia, Canada.

Address reprint requests to M.A. Sargent, MD, Department of Radiology, Children's and Women's Health Centre of British Columbia, 4500 Oak Street, Vancouver, British Columbia V6H 3N1, Canada.

partial asphyxia and is thought to occur because of disturbances in cerebral perfusion, principally affecting the boundary zones of the cortex and the subcortical white matter.

The second pattern is of injury to the thalami and basal ganglia, with relative preservation of the cerebral cortex. This central pattern of hypoxic-ischemic encephalopathy has been variously referred to as the syndrome of acute near-total intrauterine asphyxia, profound asphyxia, or the deep nuclear brain stem variety of selective neuronal necrosis (4–6). It is typically associated with acute, relatively brief, intrapartum events such as placental abruption. The result of the rapid insult is selective injury to the more metabolically active central structures, particularly the ventrolateral thalami, posterior lentiform nuclei, and perirolandic cortex. The affected sites correlate with areas of primary myelination (7).

MR imaging performed in the subacute phase 1 to 3 weeks after the acute central pattern of hypoxic-ischemic encephalopathy typically shows abnormal T1 hyperintensity in the ventrolateral thalami, posterolateral lentiform nuclei, and perirolandic cortex. Hippocampal lesions also are found in these cases (8–10). Late follow-up imaging reveals atrophy and MR signal intensity abnormalities in similar locations, and calcification may be present in the thalami. Imaging correlates of brain stem injury are infrequently observed (5, 11), but animal models and pathologic specimens confirm that acute asphyxia injures the brain stem (12, 13).

Although pathologic evidence of cerebellar injury in full-term neonates with hypoxic-ischemic encephalopathy is well recognized, cerebellar injury has not generally been identified by means of neuroimaging. Because the cerebellar vermis is also one of the more metabolically active sites in the brain of the term neonate, we hypothesized that imaging evidence of cerebellar injury should be expected in neonates with the acute central form of hypoxic-ischemic encephalopathy. In support of this hypothesis, we observed cerebellar vermian atrophy on follow-up imaging studies performed at our own institution and elsewhere of several patients who had evidence of thalamic injury after neonatal hypoxic-ischemic encephalopathy.

Both the cortical and the central patterns of neonatal hypoxic-ischemic injury may be recognized on CT scans obtained at the anticipated time of maximal cerebral edema when the patient is approximately 3 days old (14–16). In the cortical pattern, diffuse edema of the cerebral cortex can be seen with normal thalami and basal ganglia. On the other hand, the central form of injury is characterized by thalamic edema with relatively normal cortex. In our experience, involvement of the lentiform nuclei is less discernible than is thalamic edema. The perirolandic and hippocampal injuries associated with acute central hypoxic-ischemic encephalopathy may not be visible on the neonatal CT scan. Hence, in this article, reference to "thalamic edema with cortical sparing" implies that no evidence of diffuse cerebral cortical edema is observed but rolandic and hippocampal injury may be present.

Both the cortical and central patterns of injury may occur concurrently, such that edema affects all the supratentorial brain, possibly related to both the duration and the severity of the hypoxic-ischemic insult. We previously found that 31 of 100 3-day-old patients with clinical neonatal hypoxic-ischemic encephalopathy had thalamic edema shown by CT (15). Thalamic edema was associated with an adverse prognosis. Twenty-one of the 31 neonates had combined thalamic and cortical edema, and 10 had thalamic edema with cortical sparing.

The primary purpose of this study was to document the occurrence of vermian atrophy in patients who sustain neonatal hypoxic-ischemic encephalopathy. We anticipated that cerebellar injury would be more likely to occur after the acute central form of hypoxic-ischemic encephalopathy; we therefore selected the imaging studies that were performed at our institution of pediatric patients who had thalamic edema shown by neonatal CT. Our secondary aims were to verify that thalamic edema shown by neonatal CT is an indicator of permanent thalamic injury and to assess the late cerebral cortical changes associated with neonatal CT evidence of thalamic injury.

Methods

This retrospective study was performed at a tertiary care children's hospital. CT scans obtained at our institution of neonates with clinically diagnosed hypoxic-ischemic encephalopathy during a period of 13 years were retrospectively reviewed by one of the authors (K.J.P.). The CT scans were 5-mm axial view scans obtained through the brain without contrast enhancement at 72 ± 12 hr of life in all cases. Each CT study was performed immediately after the scanner was calibrated to a water phantom, and the CT measurements were accurate to ±2 H. Thalamic edema was diagnosed if the thalamic attenuation was visually equal to or less than that of the adjacent white matter. For the purpose of this study, equivocal cases were not included. Fifty-five term neonates with thalamic edema were identified.

Each neonatal CT scan was reviewed to determine whether associated diffuse cerebral cortical edema was present. Diffuse cerebral cortical edema was diagnosed if the cerebral cortical gray matter was of similar attenuation to that of underlying white matter with loss of the gray matter "ribbon" over 50% of the cortex. Typically, >75% was involved. Cerebral edema was determined to be absent ("cortical sparing") if edema was evident over <25% of the cortex. Typically, <10% was involved. For the purpose of this study, equivocal cases with edema of 25% to 50% of the cerebral cortex were excluded.

Cerebellar edema shown by neonatal CT was diagnosed if the cerebellar cortical gray matter attenuation was visually equal to that of the cerebellar white matter. It was considered equivocal if the cerebellar cortical gray matter attenuation was visually between that of white matter and normal cortical gray matter.

Additional neonatal neuroimages of the 55 patients, including 33 neurosonograms obtained at 1 to 2 days and seven MR images obtained at 10 to 18 days, were also reviewed. Neurosonography was performed by using 5- or 7-MHz transducers, with conventional coronal and parasagittal views obtained through the anterior fontanelle and a view of the cerebellum obtained through the posterolateral fontanelle. Neonatal MR imaging included spin-echo T1-weighted (800/20 [TR/TE]),

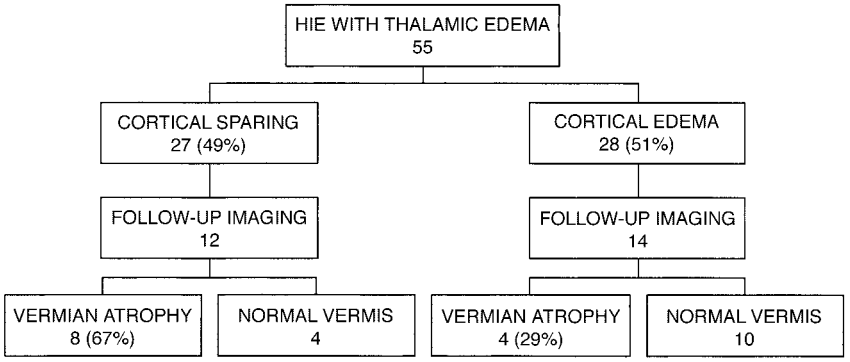

FIG 1. Schematic diagram shows frequency of vermian atrophy in children after neonatal hypoxic-ischemic encephalopathy with thalamic edema.

fast spin-echo T2-weighted (3555/80; echo train length, 8 ms), inversion recovery T1-weighted (2091/30; inversion time, 1100 ms), and spin-echo proton density–weighted and T2-weighted (3000/60,120) sequences. The MR images were reviewed for evidence of thalamic, cerebellar, and cortical signal intensity abnormalities and were correlated with the neonatal CT scans and with follow-up studies.

Follow-up imaging studies were performed at the request of the patients' individual physicians and were not routinely done. Hence, follow-up studies were available for only 26 of the 55 cases. Indications for requesting the 26 follow-up examinations were multiple and included neonatal hypoxic-ischemic encephalopathy (14 cases), infantile spasms (two cases), seizures (seven cases), cerebral palsy (six cases), developmental delay (four cases), choreoathetosis (one case), and microcephaly (one case); indications were unavailable in four of the 26 cases.

The follow-up imaging studies were reviewed separately without knowledge of the findings of neonatal imaging. They included 17 CT scans and 13 MR images of the brain of 26 patients. Four patients had both CT scans and MR images available. The CT scans and MR images were obtained at median ages of 10 months (range, 4–107 months) and 19 months (range, 5–49 months), respectively. To allow good demonstration of myelination on T2-weighted images, elective MR images were obtained at an older age than were elective CT scans. The CT scans were 5-mm axial scans obtained through the brain, and the MR images included combinations of spin-echo T1-weighted (600/16) and fast spin-echo T2-weighted (3555/80–112; echo train length, 8) sequences obtained in at least two planes, with T1-weighted inversion recovery (2140/30; inversion time, 600 ms) or volumetric steady-state T1-weighted gradient-echo (22/4.4; flip angle, 30 degrees) images in selected cases. With follow-up studies, the cerebellum was visually assessed for evidence of vermian or hemispheric atrophy and the cortex and basal ganglia were assessed for atrophy, abnormal CT attenuation, and abnormal MR signal intensity.

The initial selection of the cases for this study was determined by one pediatric neuroradiologist (K.J.P.), whereas all the neuroimaging studies in the 55 study cases were reviewed independently by two pediatric neuroradiologists (K.J.P., M.A.S.). For any disagreement between the two observers, consensus was reached by joint review.

Autopsy was performed in four of the 55 patients. Three of these four neonates had died at 4 days old and one at 16 days old. In each case, the brain and spinal cord were fixed in 10% neutral buffered formalin for 2 weeks before examination and sectioning. Sections from one of the frontal, parietal, temporal, and occipital lobes, the thalami, basal ganglia, hippocampi, cerebellar hemispheres, midbrain, pons, medulla, cervical, thoracic, and lumbosacral spinal cord were taken for examination. The cerebellar vermes were sectioned in three of four cases, and 6-μm sections were stained with hematoxylin and eosin. The histologic findings of the brain and spinal cord were retrospectively reviewed by a pediatric neuropathologist and were compared with the findings described in the original autopsy reports.

The cohort of participants was divided into two groups on the basis of neonatal CT findings. The first group had thalamic edema with cortical sparing, and the second group had combined thalamic and diffuse cerebral cortical edema. The proportions of patients who developed cerebellar vermian atrophy were calculated for the two groups, and the 95% confidence limits for the proportions were obtained from standard scientific tables. Statistical analysis was performed by comparison of the proportions of patients with cerebellar atrophy in the two groups by using a significance level of $P < .05$.

Results

Of the 55 neonatal CT scans, 27 (49%) showed thalamic edema with cortical sparing and 28 (51%) showed thalamic edema with diffuse cortical edema. Among the 26 patients who underwent follow-up imaging, 12 had thalamic edema with cortical sparing and 14 had thalamic edema with diffuse cortical edema (Fig 1). Abnormalities in the thalami, including atrophy, increased attenuation, calcification, and MR signal intensity changes, were found in 25 of the 26 patients with follow-up neuroimages.

The indications for and findings of imaging of the 26 patients who had follow-up studies are summarized in Tables 1 and 2. Among these patients, the vermes shown on the neonatal CT scans were normal in 23 cases, equivocal for edema in three cases, and not definitely abnormal in any case. On neonatal CT scans, the cerebellar hemispheres were normal in 15 cases, equivocal for edema in seven, and considered to show definite edema in four. No cerebellar abnormalities were shown by neonatal neurosonography. None of the patients had cerebellar hemorrhage. Cerebellar edema shown by neonatal CT did not correlate with the presence of cerebellar atrophy shown by follow-up imaging.

MR imaging was performed when the neonates were between 10 and 18 days of age in seven cases. In all seven cases, thalamic edema with cortical sparing was shown by initial CT and the cerebellar vermes and hemispheres appeared normal. Abnormal T1 or T2 signal intensity was present in the ventrolateral thalami in all seven cases and in the posterior lentiform nuclei (6), rolandic cortex (4), and hippocampi (3).

On late follow-up neuroimages obtained at 4 to 80 months of age, 12 (46%) of 26 patients (95% confi-

TABLE 1: Neonatal and late imaging findings for children who had neonatal thalamic edema with cortical sparing

Patient No.	Follow-up Age in Months (CT/MR Imaging)	Indications Given for Follow-up Imaging	Neonatal CT: Cerebellar Vermis	Neonatal CT: Cerebellar Hemispheres	Follow-up Imaging: Cerebellar Vermis	Follow-up Imaging: Cerebellar Hemispheres	Follow-up Basal Ganglia*	Follow-up Cerebral Cortex	Follow-up Cerebral White Matter
1	NA/19	Perinatal asphyxia	Normal	?Edema	Superior vermis atrophy	Normal	Thalami, lentiforms	Hippocampi, ?Rolandic	Rolandic
2	5/5	Infantile spasms	?Edema	Normal	Superior vermis atrophy	Normal	Thalami, lentiforms	?Rolandic	Rolandic
3	10/19	Spastic quadriplegia, seizures	Normal	Normal	Superior vermis atrophy	Normal	Thalami, lentiforms	Normal	Periventricular
4	NA/24	Neonatal HIE, cerebral palsy	Normal	Normal	Superior vermis atrophy	Normal	Thalami	Normal	Normal
5	5/8	Developmental delay, spastic quadriplegia	Normal	Normal	Superior vermis atrophy	Normal	Thalami, lentiforms	Normal	Periventricular, Rolandic
6	NA/12	Cerebral palsy	?Edema	Normal	Normal	Normal	Thalami, lentiforms	Rolandic, ?hippocampi	Periventricular, Rolandic
7	NA/15	HIE follow-up	Normal	Normal	Superior vermis atrophy	Normal	Thalami, lentiforms	Rolandic, ?hippocampi	Periventricular, Rolandic
8	4/NA	Asphyxia follow-up	Normal	Normal	Superior vermis atrophy	Normal	Thalami	Global	Global
9	6/NA	NA	Normal	Edema	Normal	Normal	Thalami, lentiforms	Normal	Periventricular
10	24/NA	Developmental delay, cerebral palsy	Normal	Edema	Superior vermis atrophy	Normal	Thalami	Normal	Normal
11	21/36	Choreoathetosis	Normal	Normal	Normal	Normal	Thalami, lentiforms	Normal	Periventricular
12	NA/27	NA	Normal	Normal	Normal	Normal	Thalami	Rolandic	Rolandic

Note.—NA indicates not applicable because procedure not performed; ?, equivocal; HIE, hypoxic-ischemic encephalopathy; Global, generalized abnormality. Note that anatomic sites as listed under Follow-up Imaging had one or more of the following: atrophy, abnormal MR imaging signal, or abnormal CT attenuation.

* Caudate nuclei were not separately assessed.

dence interval, 27–65%) were found to have cerebellar vermian atrophy (Fig 1). These 12 cases represent 22% of the original cohort of 55 neonates. Vermian atrophy in each case mainly affected the superior vermis. Mild symmetric cerebellar hemispheric atrophy was observed in one of the 12 patients with vermian atrophy. No patient had cerebellar hemispheric atrophy without vermian atrophy. Vermian atrophy was present in eight (67%) of 12 patients who had neonatal thalamic edema with cortical sparing, compared with four cases among 14 (29%) in patients who had combined thalamic and cortical edema. The difference in the frequency of vermian atrophy in the two groups approached but did not reach statistical significance (χ^2 test for the equality of two binomial proportions: with Yates correction for small sample, $P = .12$; without Yates correction, $P = .05$). Two of the seven patients with normal vermes shown by MR imaging during the neonatal period had vermian atrophy shown by late follow-up imaging; the remaining five did not undergo follow-up imaging.

Superior vermian atrophy in these cases was shown by using CT, MR imaging, or both. In all four patients who underwent both follow-up CT and follow-up MR imaging, the findings of the two modalities agreed (three with and one without vermian atrophy). The characteristic feature on axial view CT scans was focal reduced attenuation in the position of the superior vermis, often with visible volume loss (Fig 2). Typical features of superior vermian injury on MR images included hyperintensity on T2-weighted images, with volume loss shown in orthogonal planes (Figs 3 and 4). T2 hyperintensity appeared to be due to a combination of increased CSF volume with abnormal intrinsic vermian signal intensity. In the midline sagittal view MR images, the vermian tissue loss appeared to be deep rather than peripheral (Fig 5).

Late MR images were obtained for eight of the 12 patients with vermian atrophy. All eight had signal intensity abnormalities in the thalami. Among these eight, localized atrophy of the rolandic cortex was present in four, normal cortex was shown in three, and asymmetric cortical atrophy was observed in one. Late MR images were obtained for five of the 14

TABLE 2: Neonatal and late imaging findings for children who had neonatal thalamic edema with cortical edema

Patient No.	Follow-up Age in Months (CT/MR Imaging)	Indications Given for Follow-up Imaging	Neonatal CT: Cerebellar Vermis	Neonatal CT: Cerebellar Hemispheres	Follow-up Imaging: Cerebellar Vermis	Follow-up Imaging: Cerebellar Hemispheres	Follow-up Basal Ganglia*	Follow-up Cerebral Cortex	Follow-up Cerebral White Matter
13	NA/7	Severe HIE, seizures	Normal	?Edema	Superior vermis atrophy	Normal	Thalami, lentiforms	Rolandic	Global
14	NA/7	Neonatal HIE, infantile spasms	Normal	?Edema	Normal	Normal	Lentiforms, ?thalami	Global	Global
15	13/NA	Seizures	Normal	?Edema	Normal	Normal	Thalami, lentiforms	Global	Global
16	13/NA	NA	Normal	Edema	Normal	Normal	Thalami	Global asymmetric	Global asymmetric
17	5/NA	Birth asphyxia	Normal	Normal	Normal	Normal	Thalami, lentiforms	Global	Global
18	107/NA	Follow-up neonatal IVH and infarction	?Edema	Edema	Normal	Normal	Thalami, lentiforms asymmetric	Global	Global
19	4/NA	Follow-up HIE, developmental delay	Normal	?Edema	Superior vermis atrophy	Normal	Thalami, ?lentiforms	Normal	Global
20	13/NA	NA	Normal	Normal	Normal	Normal	Thalami, ?lentiforms	Rolandic	Global
21	15/NA	Seizures, microcephaly, spastic cerebral palsy	Normal	?Edema	Normal	Normal	Thalami, lentiforms	Global	Global
22	80/NA	Developmental delay, seizures	Normal	Normal	Superior vermis atrophy	?Atrophy	Asymmetric thalami, lentiforms	Asymmetric Lt global, Rt Rolandic	Asymmetric Lt global
23	5/NA	NA	Normal	?Edema	Normal	Normal	Asymmetric lentiforms, thalami	Asymmetric global	Asymmetric global
24	NA/49	Follow-up HIE	Normal	Normal	Normal	Normal	Normal	Posterior	Posterior
25	5/NA	Follow-up HIE	Normal	Normal	Normal	Normal	Thalami, lentiforms	Asymmetric global	Asymmetric global
26	NA/25	Follow-up neonatal HIE seizures	Normal	Normal	Superior vermis atrophy, ?inferior vermis atrophy	Normal	Thalami, lentiforms	Rolandic	Global

Note.—NA indicates not applicable because procedure not performed; HIE, hypoxic-ischemic encephalopathy; ?, equivocal; IVH, intraventricular hemorrhage; Global, generalized abnormality. Note that anatomic sites as listed under Follow-up Imaging had one or more of the following: atrophy, abnormal MR imaging signal, or abnormal CT attenuation.

* Caudate nuclei were not separately assessed.

patients who did not have vermian atrophy. The thalami were abnormal in four of the five. The cerebral cortex showed focal rolandic atrophy in two, normal cortex in one, and generalized cortical atrophy in one. One patient with both thalamic and cortical edema during the neonatal period had normal thalami with posterior cortical atrophy shown by late MR imaging.

Among 12 patients who had neonatal thalamic edema with cortical sparing, follow-up CT or MR imaging showed normal cortex or localized rolandic atrophy in 11 cases (92%) and generalized cortical atrophy in one. White matter abnormalities were relatively mild and seen in the periventricular area or extending to the rolandic cortex. Among the 14 patients who had combined thalamic and cortical edema in the neonatal period, follow-up imaging showed generalized cortical atrophy in eight (57%), localized rolandic atrophy in four, posterior atrophy in one, and normal cortex in one. White matter atrophy was seen in all 14 cases. Multicystic encephalomalacia was not shown in any of the 26 cases with follow-up imaging.

Autopsy was performed in four neonates from the initial series of 55. On CT scans obtained in each of these four neonates at 3 days old, the vermes appeared normal; two were shown to have mild edema of the cerebellar hemispheres. Three of the four cases had CT evidence of thalamic edema with cortical sparing, and one had combined thalamic and cortical edema. Gross examination of the neonate who survived to 16 days showed that the brain and spinal cord were normal, whereas the three neonates who survived only 4 days were shown to have cerebral edema. The hematoxylin and eosin–stained specimens showed

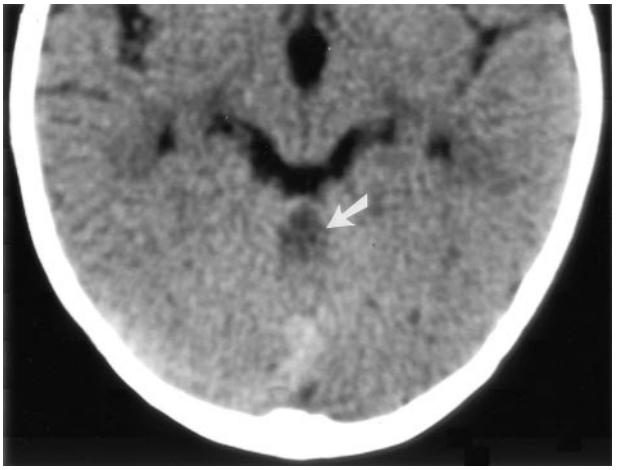

FIG 2. Axial view CT scan obtained through the posterior fossa in a 10-month-old female infant (patient 3), who was born before arrival at the hospital, shows focal hypoattenuation in the superior vermis (*arrow*). The thalami were small but with normal attenuation (not shown). This patient had thalamic edema with normal cortex shown by neonatal CT.

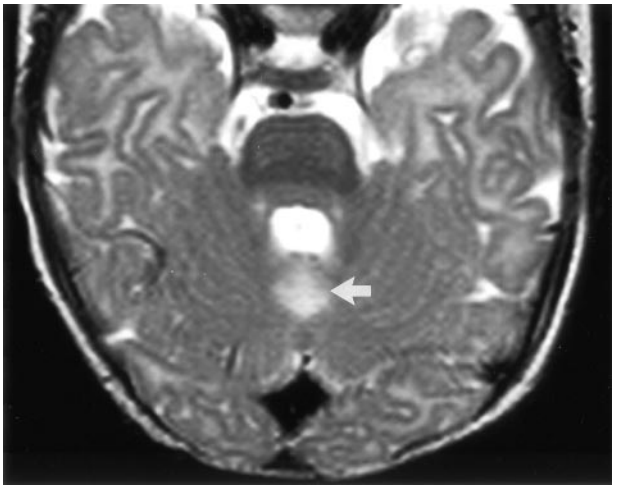

FIG 3. Axial view T2-weighted fast spin-echo (3555/112) image obtained through the posterior fossa in a 5-month-old male infant (patient 2), who was born after uterine rupture, shows hyperintensity in the cerebellar vermis immediately behind the fourth ventricle (*arrow*). Neonatal CT performed on day 3 showed abnormal thalami with normal cortex, whereas MR imaging performed on day 17 showed signal intensity abnormalities in the thalami, hippocampus, and rolandic cortex.

findings similar to those documented in the original autopsy reports. Cerebellar vermian abnormalities consistent with hypoxic-ischemic injury were found in three cases; the vermis was not examined in the fourth. Histologic abnormalities included loss of Purkinje cells, eosinophilic Purkinje cells, and proliferation of Bergmann astrocytes (Fig 6). Three of the four neonates had cerebellar hemispheric abnormalities shown at autopsy, affecting the dentate nucleus in three and the Purkinje cells in two. Anoxic changes were shown in the thalami and hippocampus. Anoxic changes were characterized by necrosis of the neurons and eosinophilia of the neuronal cytoplasm in the three neonates who survived for 4 days. Loss of neurons, calcification, and gliosis were shown to have occurred in the neonate who survived for

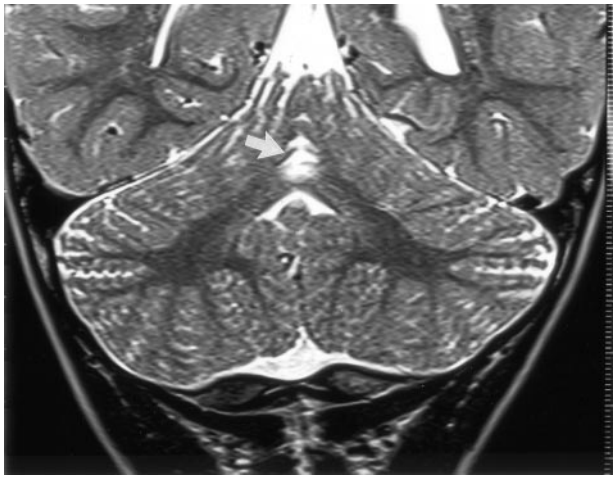

FIG 4. Coronal view T2-weighted fast spin-echo (6480/96) MR image of a 20-month-old boy (patient 5) shows hyperintensity with volume loss in the superior cerebellar vermis (*arrow*). This child had thalamic edema with normal cortex shown by neonatal CT. Other images in this follow-up study showed symmetrical hyperintensity of the ventrolateral thalami, posterior lentiform nuclei, and periventricular white matter extending to the rolandic cortex but with normal cortical gray matter.

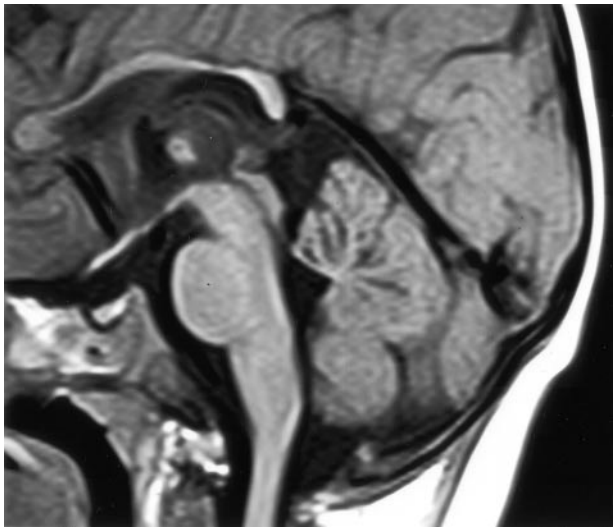

FIG 5. Midsagittal view T1-weighted (600/10) MR image of the same patient shown in Figure 2 shows volume loss centrally in the cerebellar vermis. Other findings included abnormal lentiform nuclei, signal intensity changes in the thalami, and white matter with mild atrophy of the rolandic cortex. In the midsagittal view, the corpus callosum appears thin.

16 days. Anoxic changes were shown in the cortex of three neonates. In two of the three, the motor cortex was the most severely affected. Brain stem involvement was revealed by all four autopsies.

Discussion

We have shown that neuroimaging evidence of cerebellar vermian atrophy can be seen after neonatal hypoxic-ischemic encephalopathy. We are uncertain whether vermian atrophy after neonatal encephalopathy is due to necrosis from direct hypoxic-ischemic injury or whether it is a secondary effect. Delayed cell

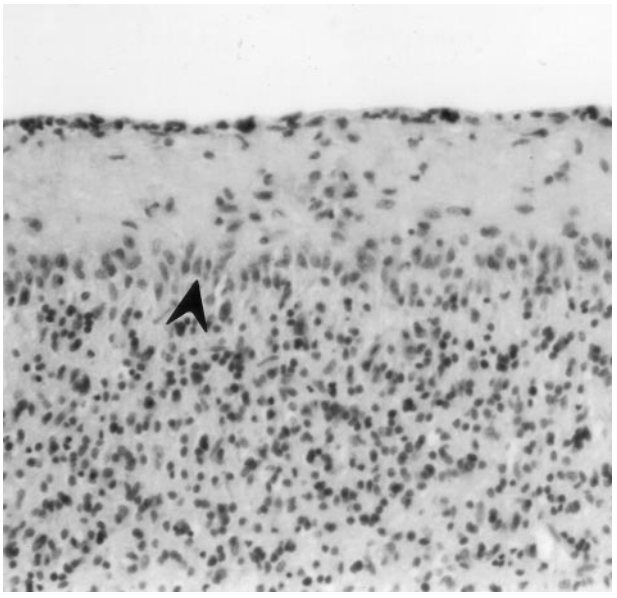

FIG 6. Cerebellar vermis of an asphyxiated twin born after cord prolapse. CT performed on day 3 showed thalamic edema without cortical involvement. The neonate died at 16 days old. Photomicrograph of the cerebellum shows loss of Purkinje cells and proliferation of Bergmann glia (*arrowhead*) (hematoxylin and eosin stain; original magnification, ×100).

death due to apoptosis contributes to injury to the cingulate cortex in both birth asphyxia and unexplained intrauterine death in humans (17). In piglets, different areas of the brain have different propensities to apoptosis (18). Asphyxia in rat pups has been shown to cause neurodegeneration by apoptosis in brain regions remote from the primary injury (19). It is possible that both neuronal necrosis and apoptosis contribute to the vermian atrophy we have observed.

Neonatal neurosonography performed during the first 3 days of life failed to disclose any cerebellar lesions, whereas findings of CT of the cerebellum in a 3-day-old patient did not correlate with subsequent cerebellar atrophy. It is intriguing that we did not find cerebellar lesions by performing conventional MR imaging in a patient approximately 10 days of age, when signal intensity abnormalities were readily shown in other affected sites. Although our neonatal MR images routinely included multiple conventional sequences, we rarely used diffusion imaging and did not use MR spectroscopy. It is possible that the timing of our MR imaging was insensitive to vermian changes. Another group was unable to show MR signal intensity abnormality in the dentate nuclei of eight neonates with severe hypoxia-ischemia who died during the first week of life, despite histologic abnormality in all eight (20). In one case report, reference was made to T2 signal intensity abnormalities of the midline cerebellum shown by MR imaging performed 25 days after acute intrapartum asphyxia (21). An example of abnormal diffusion in the vermis as shown on an MR image obtained at day 2 has been presented (22).

In all four patients from our series who underwent both follow-up CT and MR imaging, findings of the presence or absence of vermian atrophy were consistent with both techniques. Hence, we think that our data provide a good estimate of the prevalence of vermian atrophy after neonatal encephalopathy with CT evidence of thalamic involvement. We acknowledge that our data may be subject to clinical selection bias because only half of the patients in our series underwent follow-up neuroimaging. Of note is that in some of our cases with imaging evidence of the acute central pattern of hypoxic-ischemic encephalopathy, we found that superior vermian atrophy was the most easily identified abnormality on follow-up CT scans, because thalamic atrophy was subtle when normal thalamic attenuation was present.

If we assume that every patient in our series who did not have follow-up images available had a normal vermis, our conservative estimate of the prevalence of vermian atrophy after neonatal encephalopathy with thalamic edema is 22%. Because the sensitivities of neonatal CT and MR imaging may be different, the frequency of vermian atrophy found after thalamic abnormality and diagnosed on the basis of neonatal MR imaging findings may be different from the frequency found after diagnosis based on neonatal CT findings. Extrapolating previous data that report 31% of asphyxiated pediatric patients have thalamic injury shown by neonatal CT and assuming that cerebellar atrophy does not occur without thalamic injury, our minimum estimate is that 7% of all asphyxiated neonates will develop vermian atrophy (15).

Radiologic evidence of cerebellar injury after neonatal hypoxic-ischemic encephalopathy has previously been considered rare. Among 104 patients with MR imaging evidence of hypoxic-ischemic brain damage, 73 of whom had periventricular leukomalacia, only one was listed as having evidence of unspecified cerebellar or brain stem injury. The single case had the basal ganglia–thalamic pattern of MR abnormality (23). Individual cases of vermian atrophy have been mentioned in other series, with predominant involvement of the superior vermis, as in our cases (7, 9, 10). Using computer quantification in children with severe basal ganglia and thalamic lesions, greater volume reduction was found in the cerebellar vermis than in the cerebellar hemispheres (24).

In the current study, we found thalamic abnormality at follow-up neuroimaging in 25 of 26 patients who had thalamic edema shown by CT performed at 3 days old. We also showed that thalamic edema correlated with findings at neonatal autopsy. Hence, we think that neonatal thalamic edema, as defined by thalamic attenuation equal to or less than that of adjacent white matter on a CT scan obtained when the patients are age 3 days, is a highly specific indicator of thalamic hypoxic-ischemic injury. In the one case in our series in which the thalamus was normal at follow-up, a posterior distribution of cortical atrophy was observed; in retrospect, it is possible that the neonatal encephalopathy was a consequence of hypoglycemia rather than hypoxia-ischemia (25).

For this study, we selected patients with thalamic edema shown by neonatal CT because we had previ-

ously observed vermian atrophy in patients with imaging evidence of thalamic injury, including some patients from other institutions that were not included in this series. Although we have not yet formally reviewed the follow-up imaging findings for asphyxiated patients with the "prolonged partial" pattern of cortical edema without thalamic edema, we are not aware of any case in which we have seen vermian atrophy in that group. This is to be the subject of further review.

In this study, we found a tendency for vermian atrophy to be more common among patients who had thalamic edema and cortical sparing, compared with patients who had both thalamic and diffuse cortical edema. The difference did not reach statistical significance, likely because of the relatively small numbers. If confirmed in larger series, we think that our radiologic observations would suggest that superior vermian atrophy is a marker of acute central rather than prolonged partial asphyxia. However, our clinical experience has shown that patients with vermian atrophy are among the most severely affected after those with neonatal hypoxic-ischemic encephalopathy, and the atrophy may also be an indicator of the severity of injury.

In summary, we have shown that cerebellar vermian atrophy develops during follow-up in a significant proportion of patients who had neonatal hypoxic-ischemic encephalopathy with CT evidence of thalamic edema. This is a new imaging sign that may be useful in evaluating CT scans and MR images of patients suspected or known to have sustained neonatal hypoxic-ischemic encephalopathy.

Acknowledgment

We thank Dr. Margaret G. Norman, who performed the original CNS autopsy examinations included in this report.

References

1. Chugani HT, Phelps ME. **Maturational changes in cerebral function in infants determined by ^{18}FDG positron emission tomography.** *Science* 1986;231:840–843
2. Kinnala A, Suhonen-Polvi H, Aarimaa T, et al. **Cerebral metabolic rate for glucose during the first six months of life: an FDG positron emission tomography study.** *Arch Dis Child* 1996;74:F153–F157
3. Ashwal S, Majcher JS, Vain N, Longo LD. **Patterns of fetal lamb regional cerebral blood flow during and after prolonged hypoxia.** *Pediatr Res* 1980;14:1104–1110
4. Martin E, Barkovich AJ. **Magnetic resonance imaging in perinatal asphyxia.** *Arch Dis Child Fetal Neonatal Ed* 1995;72:F62–F70
5. Pasternak JF, Gorey MT. **The syndrome of acute near-total intrauterine asphyxia in the term infant.** *Pediatr Neurol* 1998;18:391–398
6. Volpe JJ. **Hypoxic-ischemic encephalopathy: clinical aspects.** In: *Neurology of the Newborn.* 4th ed. Philadelphia: WB Saunders; 2001:331–394
7. Azzarelli B, Caldemeyer KS, Phillips JP, DeMyer WE. **Hypoxic-ischemic encephalopathy in areas of primary myelination: a neuroimaging and PET study.** *Pediatr Neurol* 1996;14:108–116
8. Rutherford M, Pennock J, Schwieso J, Cowan FM, Dubowitz L. **Hypoxic-ischaemic encephalopathy: early and late magnetic resonance imaging findings in relation to outcome.** *Arch Dis Child Fetal Neonatal Ed* 1996;75:F145–151
9. Maller AI, Hankins LL, Yeakley JW, Butler IJ. **Rolandic type cerebral palsy in children as a pattern of hypoxic-ischemic injury in the full-term neonate.** *J Child Neurol* 1998;13:313–321
10. Barkovich AJ. **MR and CT evaluation of profound neonatal and infantile asphyxia.** *AJNR Am J Neuroradiol* 1992;13:959–975
11. Rutherford MA. **The asphyxiated term infant.** In: Rutherford MA, ed. *MRI of the Neonatal Brain.* London: WB Saunders; 2002:99–128
12. Myers RE. **Four patterns of perinatal brain damage and their conditions of occurrence in primates.** *Adv Neurol* 1975;10:223–234
13. Volpe JJ. **Hypoxic-ischemic encephalopathy: neuropathology and pathogenesis.** In: *Neurology of the Newborn.* Philadelphia: WB Saunders; 2001:296–330
14. Lupton BA, Hill A, Roland EH, Whitfield MF, Flodmark O. **Brain swelling in the asphyxiated term newborn: pathogenesis and outcome.** *Pediatrics* 1988;82:139–146
15. Phillips RR, Brandberg G, Hill A, Roland E, Poskitt KJ. **Prevalence and prognostic value of abnormal CT findings in 100 term asphyxiated newborns.** *Radiology* 1993;189P:287
16. Roland EH, Poskitt KJ, Rodriguez E, Lupton BA, Hill A. **Perinatal hypoxic-ischemic thalamic injury: clinical features and neuroimaging.** *Ann Neurol* 1998;44:161–166
17. Edwards AD, Yue X, Cox P, et al. **Apoptosis in the brains of infants suffering intrauterine cerebral injury.** *Pediatr Research* 1997;42:684–689
18. Edwards AD, Mehmet H. **Apoptosis in perinatal hypoxic-ischaemic cerebral damage.** *Neuropathol Appl Neurobiol* 1996;22:494–498
19. Northington FJ, Ferriero DM, Graham EM, Traystman RJ, Martin LJ. **Early neurodegeneration after hypoxia-ischemia in neonatal rat is necrosis while delayed neuronal death is apoptosis.** *Neurobiol Dis* 2001;8:207–219
20. Jouvet P, Cowan FM, Cox P, et al. **Reproducibility and accuracy of MR imaging of the brain after severe birth asphyxia.** *AJNR Am J Neuroradiol* 1999;20:1343–1348
21. Pasternak JF, Predey TA, Mikhael MA. **Neonatal asphyxia: vulnerability of basal ganglia, thalamus, and brainstem.** *Pediatr Neurol* 1991;7:147–149
22. Palasis S, Grattan-Smith D, Berenson F, Little SA. **Neonatal hypoxic-ischemic injury: spectrum of conventional and advanced MR imaging findings.** Presented at the Annual Meeting of the American Society of Neuroradiology, Denver, 2000
23. Sie LT, van der Knaap MS, Oosting J, de Vries LS, Lafeber HN, Valk J. **MR patterns of hypoxic-ischemic brain damage after prenatal, perinatal or postnatal asphyxia.** *Neuropediatrics* 2000;31:128–136
24. Le Strange E, Saeed N, Counsell S. **Magnetic resonance image quantification following hypoxic-ischemic injury to the neonatal brain.** Presented at the Annual Meeting of the International Society of Magnetic Resonance in Medicine, Denver, 2000
25. Barkovich AJ, Ali FA, Rowley HA, Bass N. **Imaging patterns of neonatal hypoglycemia.** *AJNR Am J Neuroradiol* 1998;19:523–528